HEFAT2010
7th International Conference on Heat Transfer, Fluid Mechanics and Thermodynamics
19-21 July 2010
Antalya, Turkey

FLOW FIELD ANALYSIS OF AIR FLOWING THROUGH FIN-AND-TUBES WITH A PAIR OF DELTA-WINGLET VORTEX GENERATOR

Seong Won Hwang[+], Hyun jung Kim[a] and Ji Hwan Jeong[*]

[+, *] Pusan National University, School of Mechanical Engineering,
Jangjeon Dong, Geumjeong Gu, Busan 609-735 Korea
Republic of,
E-mail: jihwan@pusan.ac.kr

[a]Hoseo University, Dept. of Mathematics,
Baebangmyun, Asan 336-795 Korea
Republic of,

ABSTRACT

Among tubular heat exchangers, fin-tube heat exchangers are the most widely used in refrigeration and air-conditioning equipment. The fin shape has been varied from a plain fin to a slit fin and louver fin in efforts to enhance the performance of fin-tube heat exchangers. The performance of vortex generators in the context of heat transfer augmentation has also been investigated. Recently, delta winglet vortex generators have attracted the interest of researchers, partly on the basis of experimental data showing that fin-tube heat exchangers with delta winglet vortex generators experience considerably less pressure loss than conventional fin-tube heat exchangers while the heat transfer capacity is at nearly the same level. Previous studies showed that the efficiency of the delta winglet vortex generator varies widely depending on their size and shape, as well as the locations where they are implemented. In this paper, the flow field around delta winglet vortex generators in a common flow up arrangement was analyzed in terms of flow characteristics and heat transfer using computational fluid dynamics methods. The analyses show that flow mixing due to vortices and a delay of flow separation due to flow acceleration influence the overall performance of the fins. The pressure loss of a fin having delta winglet vortex generators was evaluated to be smaller than that of a plain fin while the heat transfer performance was enhanced at high air velocity or Reynolds number.

INTRODUCTION

Fin-tube heat exchangers are widely used in chemical process plants, power plants, and home appliances including small air conditioners and refrigerators [1]. They are generally used to exchange heat between a gas and liquid. While early fin-tube heat exchangers primarily adopted plain fins, extensive research in the area of fin shape has led to substantial progress in the development of high performance fin to produce compact heat exchangers. Current compact fin-tube heat exchangers adopt a slit fin or louver fin if the working fluid is not significantly corrosive such as in the case of a hume gas.

Fin shape studies for compact heat exchanger design continue to be conducted owing to purposed related to global environmental concerns and improvement of the energy system efficiency. One notable area of research in this regard is the incorporation of vortex generators in fins. Early vortex generator research focused on the boundary layer control of air foils [2]. Vortex generators create longitudinal vortices in the main flow to re-energize the boundary layer developed adjacent to an air foil and, in turn, delay or prevent flow separation. Since the flow mixing due to vortices is beneficial with respect to heat transfer enhancement, researchers became interested in applying the vortex generator to heat exchanger fin designs. The shape of the vortex generator examined in the open literature includes a rectangular wing, rectangular winglet, delta wing, and delta winglet. Recent research concerning the effects of vortex generators on the performance of fin-tube heat exchangers has focused on a delta winglet vortex generators (DWVG) rather than other shapes.

NOMENCLATURE

a	[°]	Attack angle
A_c	[m^2]	Area of fin colloar
A_{min}	[m^2]	Area of minimum air flow
A_f	[m^2]	Area of frontal air flow

A_{fin}	[m^2]	Area of fin
b	[°]	Central angle
C_f	[-]	Frintion coefficient
C_p	[kj/kgK]	Static pressure specific heat
D	[m]	Tube diameter
D_c	[m]	Characteristic length
f	[-]	Fanning friction factor
f_v	[Hz]	Vortex shedding frequency
g	[m]	Between tube and winglet gap
h	[W/m^2K]	Heat transfer rate
H	[m]	Fin pitch
j	[-]	Colburn j factor
k	[W/mK]	Conductivity
L	[m]	Length of heat exchanger
P	[pa]	Pressure
Q	[W]	Total heat flow
t	[s]	Time
T	[K]	Temperature
T_c	[K]	Temperature of fin collar
T_{in}	[K]	Inlet mean temperature
T_{out}	[K]	Outlet mean temperature
u	[m/s]	Velocity of x-axis
U	[m/s]	Frontal fluid velocity
v	[m/s]	Velocity of y-axis
V_{max}	[m/s]	Maximum velocity
w	[m/s]	Velocity of z-axis
W	[m]	Width of heat exchanger
W_h	[m]	Winglet height
W_l	[m]	Winglet length
α	[m^2/s]	Thermal diffusivity
δ	[-]	Boundary layer thickness
μ	[Ns/m^2]	Dynamic viscosity
ρ	[kg/m^3]	Density
υ	[m^2/s]	Kinetic viscosity
Nu	[-]	Nussrlt number
Pr	[-]	Prandtl number
Re	[-]	Reynolds number
S	[-]	Strouhal number
St	[-]	Stanton number

The vortex generators incorporated in fin-tube heat exchangers can be categorized in accordance with their configuration with respect to heat transfer tubes: 'common flow down' and 'common flow up' configurations. These configurations are illustrated in Fig. 1. A pair of vortex generators mounted behind a tube (at the downstream) is referred to as a common flow down configuration. Fiebig [3] contended that the common flow down configuration would delay flow separation and reduce drag. In the common flow up configuration, a pair of vortex generators is installed in front of the tube (at the upstream). Torii et al. [4] speculated that this configuration generates flow acceleration between a tube and vortex generators and delays flow separation and, in turn, reduces the wake region behind the tube.

The effects of vortex generators on the performance of the heat transfer surface have been investigated in recent decades. Jacobi and Shah [5] reviewed previous works carried out up to the early 1990s. In this review they explained physical phenomena and characteristic of vortices associated with vortex generators on a fin and introduced experimental and analytical results on the performance of heat exchangers having vortex generators. They categorized the vortex generators into active and passive methods depending on how vortices are created. Active methods generate vortices using external energy, such as an electric field, acoustic field, mechanical device, or surface

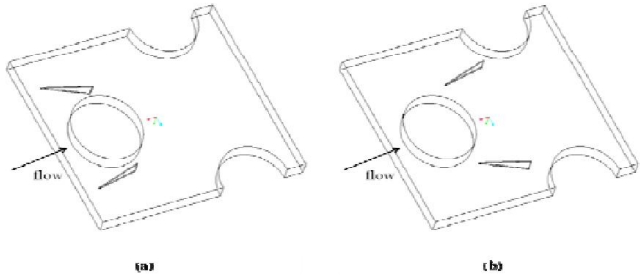

Figure 1 Configuration of vortex generator (a) common flow up, (b) common flow down

vibration. In passive methods, vortices are generated by structures and additional fluids. Regardless of the methods, it has been demonstrated that vortex generators enhance heat transfer and a simultaneous pressure drop due to form loss. An interesting characteristic of the vortex generator is that the pressure loss increase is not large compared with other interrupted fin designs. In this regard, most previous works have focused on quantification of the improvement of heat transfer performance and additional pressure drop characteristics.

Fiebig et al. [6] experimentally studied heat transfer performance in a channel with vortex generators in a common flow down configuration. The authors reported that the DWVG increases convective heat transfer by developing a boundary layer, swirl or vortices, and through flow destabilization or turbulence intensification. Their experimental data showed that the delta winglet enhances heat transfer more than a rectangular winglet. They reported obtaining the highest heat transfer coefficient at a 45° attack angle, which is defined as the angle between the flow direction and vortex generators. The effects of the vortex generators on fin-tube heat exchangers were also experimentally investigated. The authors installed 3 DWVG onto three row fin-tube heat exchangers in a common flow down configuration. They compared the effect of tube arrays, staggered and inline, on the thermal-hydraulic performance of the DWVG. The comparison showed that the f-factor of the staggered array was smaller than that of the inline array in a range of Re>1300 while nearly the same heat transfer coefficient was measured. The authors noted that DWVG have the potential to reduce the size and mass of a heat exchanger for a given heat load.

Kwak et al. [7] measured the heat transfer coefficient and pressure drop in 2, 3, 4, and 5 row fin-tube heat exchangers with a common flow up configuration DWVG in a range of 280<Re<2400. The DWVG were only mounted on the first row. Compared with plain fin heat exchangers, the DWVG fin heat exchangers showed a 10% increase in heat transfer performance in terms of j-factor for all heat exchangers and a 0~10% increase in f-factor for the 2, 4, and 5 row heat exchangers. For the 3 row heat exchanger, however, the f-factor was dramatically decreased by 30~50%. The authors attributed this to the effects of vortices, which were produced at the first row of the tube but did not reach the fourth and fifth rows.

The effect of the number of DWVG rows was investigated by Kwak et al. [8]. They measured the heat transfer capacity and pressure drop of staggered array fin-tube heat exchangers

that were identical except for the number of DWVG rows. The heat exchanger with a single row of DWVG experienced 10~30% larger heat transfer capacity and 34~55% less pressure drop than the heat exchanger without DWVG. For the heat exchanger with two rows of DWVG, however, the heat transfer capacity increased by 6~15% and the pressure drop also increased by 61~117% compared with the heat exchanger with a single row of DWVG. The authors contended that the DWVG in the second row obstructed the air flow and decelerated it to produce an additional pressure drop.

The brief review provided above shows that previous research has largely focused on the quantitative and qualitative effects of vortex generators on pressure drop and heat transfer performance, regardless of whether an experimental or numerical approach was taken. Previous works have commonly verified that the vortex generators enhance heat transfer. However, there is less consistency with respect to the pressure drop penalty. This reflects a lack of phenomenological understanding as to how vortex generators influence the heat transfer performance and pressure drop, as little research has been devoted to the underlying mechanism. In this regard, the present work aims to arrive at a better phenomenological understanding of how the DWVG enhances heat transfer performance with a relatively small pressure drop penalty and sometimes even a reduced penalty. To this end, computational fluid dynamics (CFD) analyses are carried out to obtain information on the fluid flow and heat transfer in a fin-tube heat exchanger with DWVG.

FLUID FLOW AND CONVECTIVE HEAT TRANSFER

Fluid flow in a channel is analyzed by the Navier-stokes equations, which describe the motion of an incompressible Newtonian fluid [9]. In order to analyze the flow field and temperature field, we need a set of differential equations consisting of the mass conservation equation, momentum conservation equation, and energy conservation equation.

Mass conservation equation (Continuity equation)

$$\nabla \cdot (\rho V) = 0 \tag{1}$$

Momentum conservation equation (Navier-stokes equation)

$$\frac{\partial \rho V}{\partial t} + (\rho V \cdot \nabla V) = -\nabla P + \mu \nabla^2 V \tag{2}$$

Energy conservation equation

$$\rho C_p \left(\frac{\partial T}{\partial t} + V \cdot \nabla T\right) = k\ \nabla^2 T \tag{3}$$

where, V, ρ, t, P, μ, T, k, and C_p represent the velocity, density, time, pressure, dynamic viscosity, temperature, thermal conductivity, and constant-pressure specific heat [10]. Since the above equations are non-linear they are usually solved using a numerical method in order to determine the velocity field and temperature field in a flow passage. An air flow passing around a circular tube will be influenced by various factors. When the flow velocity is very low (Re<<1), the flow is dominantly affected by inertial force and maintains a normal stream at the back of the tube. In a range of 50>Re, the viscous force of the fluid rather than the inertial force has a prevailing impact on the air flow. As a result, an adverse pressure gradient may develop leading to a flow separation from the tube where a smoothly changing stream line no longer persists. When the flow separation occurs, a wake develops in the rear of the tube where the flow swirls and does not mix with external flow. This wake is usually detrimental to heat transfer in terms of heat transfer capacity and pressure loss [9].

When a flow over a flat plate is considered, the above conservation equations may be represented in a two-dimensional form. In this case, equation (2) can be written as follows:

$$\rho\left(u\frac{\partial u}{\partial x} + v\frac{\partial u}{\partial y}\right) = -\frac{\partial p}{\partial x} + \frac{\partial^2 u}{\partial y^2} \tag{4}$$

where u and v are velocity components in the x and y directions, respectively. Note that the velocities in the x and y directions are zero at a wall: that is, $u = v = 0$ at $y = 0$. This is called a no-slip condition. We can derive a solution to equation (4) with some boundary conditions that are applicable to a boundary layer including a zero pressure gradient along the flow direction ($\partial p / \partial x = 0$) as follows:

$$\frac{u}{u_\infty} = \frac{3}{2}\frac{y}{\delta} - \frac{1}{2}\left(\frac{y}{\delta}\right)^3 \tag{5}$$

where, u_∞ and δ represent the free stream velocity and boundary layer thickness, respectively. On the other hand, the wall shear stress (τ_w) and skin friction factor ($C_f = f/4$) are related as follows:

$$\tau_w = \mu\left.\frac{\partial u}{\partial y}\right|_{y=0} = C_f\frac{\rho u_\infty^2}{2} \tag{6}$$

where μ represents the viscosity of the fluid. Combining equations (5) and (6) gives an analytic skin friction relationship with a Reynolds number ($\mathrm{Re} = \rho x u / \mu$) as follows:

$$\frac{C_f}{2} = 0.332\,\mathrm{Re}_x^{-1/2} \tag{7}$$

Equation (3) can also be treated in a similar manner to obtain the temperature profile in the temperature boundary layer as follows:

$$\frac{T - T_w}{T_\infty - T_w} = \frac{3}{2}\frac{y}{\delta_t} - \frac{1}{2}\left(\frac{y}{\delta_t}\right)^3 \tag{8}$$

where T_∞, T_w, and δ_t represent the free stream temperature, wall temperature, and thermal boundary layer thickness, respectively. On the other hand, the heat flux based on Newton's law and the heat flux given by Fourier's law at the wall can be obtained as follows:

$$q = h(T_w - T_\infty) = k_f \left.\frac{\partial T}{\partial y}\right|_{y=0} \tag{9}$$

where h and k_f represent the convective heat transfer coefficient and thermal conductivity of the fluid. Combining equations (8) and (9) and some manipulation give an analytic convective heat transfer coefficient relationship in terms of Nusselt number (Nu) as follows:

$$Nu_x = \frac{hx}{k_f} = 0.332\,\mathrm{Pr}^{1/3}\,\mathrm{Re}_x^{-1/2} \tag{10}$$

where Pr represents the Prandtl number ($=\nu/\alpha$) of the fluid. Equations (7) and (10) have similar functional forms and thus can be related via non-dimensional numbers as

$$\frac{C_f}{2} = \frac{Nu_x}{\mathrm{Re}_x\,\mathrm{Pr}} \times \mathrm{Pr}^{2/3} = St_x\,\mathrm{Pr}^{2/3} \equiv j \tag{11}$$

where St represents the Stanton number and j is called the Colburn j-factor. This relationship is called a Reynolds-Colburn analogy, and it implies an important physical characteristic of a heat transfer surface. Specifically, this analogy means that the heat transfer performance will be enhanced with an increase in the frictional pressure drop [11]. Heat transfer augmentation with a minimum pressure drop increase is preferred in enhanced heat transfer surface design [12].

NUMERICAL MODELING

In the present work a two-row fin-tube heat exchanger is considered for the numerical analysis. Fig. 2 shows the representative geometry of this heat exchanger. Delta winglet vortex generators are installed around the first row of the tube in a common flow up configuration. Notations for geometric definitions are also provided in Fig. 2. Table 1 lists the geometric values. Fin thickness, fin spacing, and tube size are similar to those of fin-tube heat exchangers that are widely used as condensers and evaporators of air-conditioners. The geometry and installed location of the delta winglet vortex generators are similar to those applied in the heat exchanger experimentally investigated by Kwak et al. [7].

In the present work, conjugate heat transfer analyses were carried out. That is, the energy equation is solved for the solid domain as well as the fluid domain. A cylindrical ring represents the heat transfer tube while a flat plate represents the

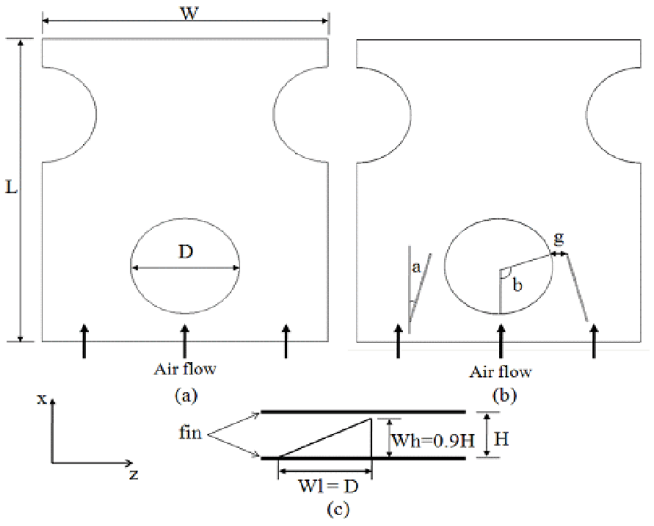

Figure 2 Definition of geometry

fin. The triangular structure located on the flat plate is the DWVG. Above these meshes for the solid part will be meshes for the fluid part (not illustrated in the Figure). Fine meshes are generated in the vicinity of the solid surface where the velocity gradient is large. The mesh size increases with increasing distance from the solid surface. To determine the size of grid, three different fluid meshes; 4.5 million, 0.75 million, and 0.23 million have been tested. The results of 4.5 million and 0.75 million meshes showed a consistent result within 2% accuracy while the result of 0.23 million meshes deviated by more than 10% from the other results. Finally 1.4 million meshes in total for the fluid domain and 0.4 million meshes for the solid part were generated and used for the present computations. The SIMPLE(Semi-Implicit Method for Pressure-Linked Equations) algorithm [13] is used to solve equation (2). Since the largest Reynolds number considered in this study is around 3000, it is not clear whether the flow is laminar or turbulent in this region. To check the flow regime, calculations using laminar and turbulent assumptions have been carried out for Reynolds

Table 1 Heat exchanger's geometry data

Notation	Meaning	Value
L	Length, (m)	0.0254
W	Width, (m)	0.021
D	Tube diameter, (m)	0.008
H	Fin pitch(m)	0.00123
Wl	Winglet length, (m)	0.00565
Wh	Winglet height, (m)	0.011
a	Attack angle, (°)	15
b	Central angle, (°)	110
g	Between tube and winglet gap, (m)	0.001

number ranging from 1600 to 3200. For the turbulent calculation, low Reynolds number k-ε model has been used. The results showed good agreement within 1% of difference in terms of friction and j-factors. As a result, laminar flow has been assumed in this paper. The boundary conditions are as follows. An inlet boundary (u = const) condition is established for the front end of the fluid domain while an outlet boundary condition is used for the rear end. The left-hand and right-hand sides are set up with a symmetric boundary condition ($w = 0$, $\frac{\partial w}{\partial z} = 0, \frac{\partial T}{\partial z} = 0$). For the solid domain, a constant temperature condition was set for the heat transfer tube inner wall. The temperature of the solid surface that is in contact with air will be numerically determined such that the heat flux through the solid part should balance with the heat flux through the air adjacent to the solid surface. Top and bottom surface set to adiabatic.[14] The air inlet temperature was fixed at 293K for all simulations. The heat transfer tube inner wall temperature was set at 333K to represent a working condition of a refrigerant condenser. The governing equations, equations (1)~(3), with these boundary conditions are numerically solved using a commercial CFD package, STAR-CD [15].

At the beginning of the CFD analyses, a preliminary calculation has been performed to determine whether the air flow in the calculation domain shows any transient behavior. Since the air velocity considered here is extremely low, the air flow is assumed to be incompressible and laminar. When fluid flows around a tube, vortex shedding may occur. If vortex shedding occurs, it is known that the Strouhal number defined by equation (15) will be 0.2 [16].

$$S = \frac{f_V D}{V} \tag{12}$$

where S, f_V, and D represent the Strouhal number, vortex shedding frequency, and tube diameter. We can then obtain the vortex shedding frequency if we substitute values of S, u, and D into equation (12). A transient simulation has been performed for two period times, but no vortex shedding was observed. Thus, only steady state calculations were performed in the following numerical simulations.

NUMERICAL RESULT

Fig. 3 shows the path lines of air, which are the trajectories that individual fluid particles follow. Air moving toward the fore-end of the heat transfer tube flows along the tube outer wall and departs from the wall and flows downstream. It is seen that this air does not contact the back side of the tube and hence there are empty regions where path lines do not pass. Some path lines contacting DWVG mounted on both sides of the tube swirl as they flow downstream. This swirl is a vortex created by the DWVG. The plot shows that the DWVG create vortices in the air flow. These vortices are expected to cause fluid mixing and promote convective heat transfer from the fin surface.

Fig. 4 shows the air flow velocity vector at the mid-plane between two fins when the frontal air velocity is 5m/s. The air enters from the right-hand side and flows around the heat transfer tube. The air flow separates from the tube wall and

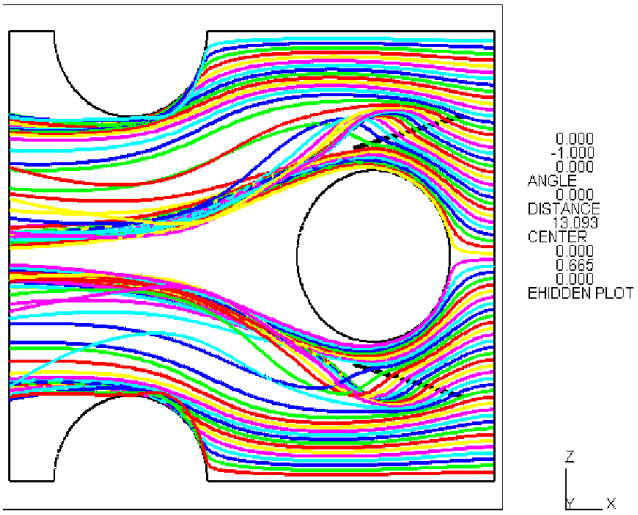

Figure 3 Fluid flow path in heat exchanger

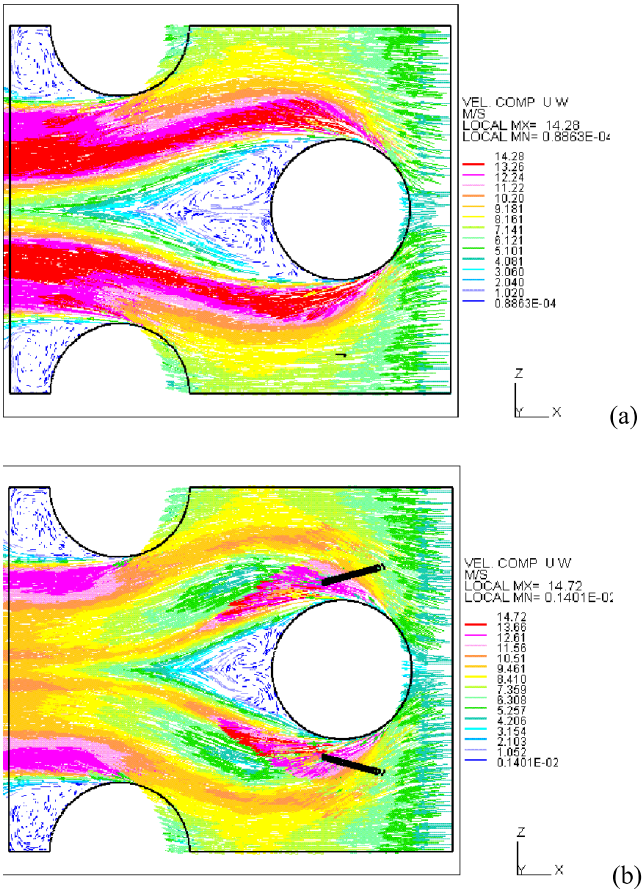

Figure 4 Air velocity vector plot at mid-plane (Re=1295, V_{max}=8.07m/s) (a) Plain fin (b) DWVG fin

develops a wake region behind the tube, where the flow slows down and circulates [11]. For a plain fin heat exchanger, as seen in Fig. 4(a), the wake is wide and extends to the tailing edge of the fin. For a DWVG fin, as seen in Fig. 4(b), the flow

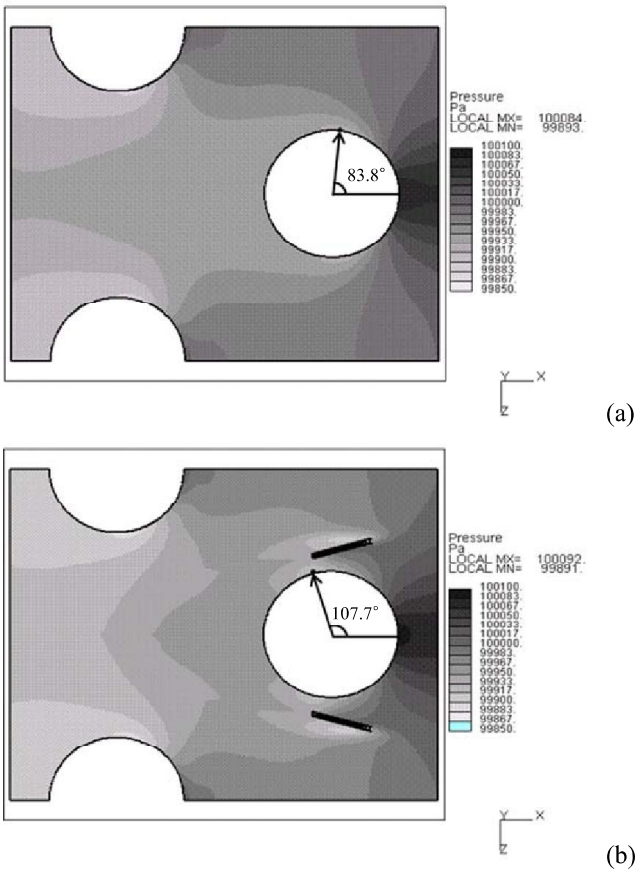

Figure 5 Static pressure contour at mid-plane and the adverse pressure point on the cylinder (Re=1295, V_{max}=8.07m/s) (a) Plain fin (b) DWVG fin

velocity increases between the DWVG and the heat transfer tube and the flow separation point moves to the rear side of the tube but it is narrower and shorter than that in the plain fin heat exchanger. The wake region appears to be extended lengthwise to the middle of the 2nd row of tubes. Fig. 4(b) shows that the air flow is accelerated between the DWVG and tube wall and consequently formation of an adverse pressure gradient is delayed and the flow separation occurs further downstream. It is believed that this delayed flow separation diminishes the wake region and makes the overall velocity profile more uniform.

The static pressure contour for the same case is shown in 5. The arrows in these plots indicate the adverse pressure gradient points where the pressure becomes minimum on the cylinder wall. The location of flow separation in the downstream is mainly affected by this point. As can be seen in the plots, the static pressure at the tube wall decreases proceeding from the fore-end of the tube to the arrow-head. However, the static pressure recovers at positions further toward the rear. Fig. 5 shows that the adverse pressure gradient point is influenced by the DWVG. The adverse pressure gradient point of the plain fin occurs at around 84° while that of the DWVG fin occurs at around 108° from the tube fore-end. This change in the adverse pressure gradient point influences the variation of the wake region, as shown in Fig. 4.

Fig. 6 shows the temperature distribution of air when its frontal velocity is 5m/sec. The plane shown in this plot represents the mid-plane between two adjacent fins. Fig. 6(a) shows that the temperature of the wake region of the plain fin This is caused by the swirling characteristic of the wake, as can be seen in the velocity vector plot of Fig. 4. When DWVG are mounted on the plain fin, however, this high temperature region is reduced, as shown in Fig. 6(b). As mentioned previously, this is caused by a reduction of the wake region due to the DWVG. The contour pattern of the air temperature distribution is quite similar to the velocity vector plot shown in Fig. 4. This is because the air temperature is directly associated with convective heat transfer, and the convective heat transfer is controlled by the air flow itself. Early researchers of convective heat transfer proved that the convective heat transfer is a function of Reynolds number (Re) and Prandtl number (Pr). This explains why the air temperature distribution of the DWVG fin heat exchanger, Fig. 6(b), appears to be more uniform than that of the plain fin heat exchanger. In order to provide a clear illustration of this, the temperature and velocity variation along the central line across the second row of the tube are plotted in Fig. 8. Fig. 8 shows that the DWVG results in a flatter temperature and velocity profiles at the rear of the heat transfer tube. The surface temperature distributions of the DWVG fin and plain fin are shown in Fig. 7. Both corners of the front end show low temperature due to the higher heat transfer rate resulting from the higher velocity compared to the

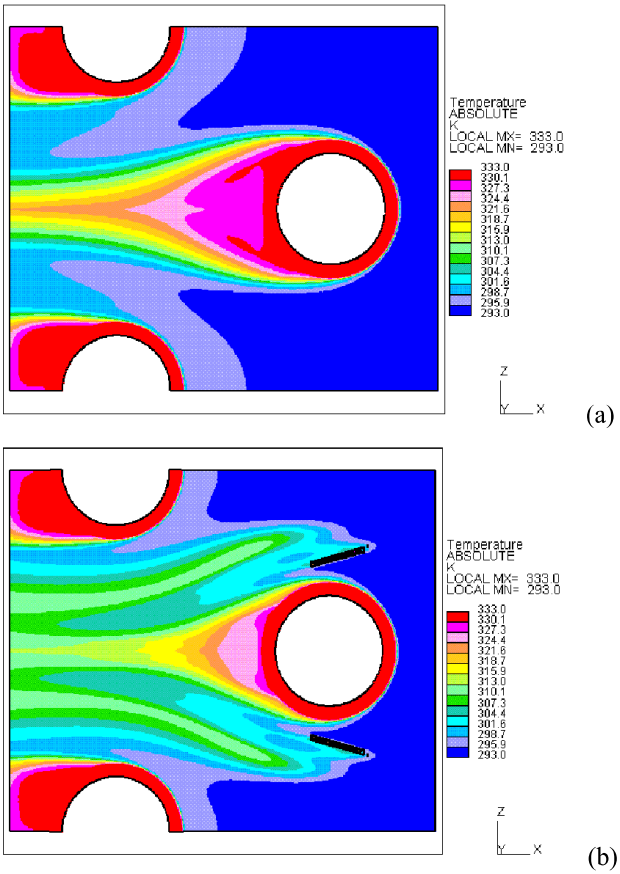

Figure 6 Temperature of air at mid-plane (Re=1295, V_{max}=8.07m/s) (a) Plain fin (b) DWVG fin

central region. As the location becomes closer to the tube, the temperature of the fin surface rises due to the conduction of heat through the fin itself. The surface temperature is evaluated to be lower moving away from the tube and the air velocity becomes higher. As noted above, the heat transfer performance in the wake region is poor. Consequently, the fin surface temperature appears to be high in the rear of the heat transfer tubes. Fig. 8 shows that this high temperature region at the back of tubes extends toward the rear end of the fin. The temperature levels around the second row tubes of the plain fin and DWVG fin are quite similar. However, those around the first row tubes show a large difference due to the influence of the DWVG. The temperature level at the back of the first row tube of the DWVG fin was evaluated to be lower than that of the plain fin. This is because the DWVG reduce the wake region and facilitate air mixing, resulting in enhanced heat transfer. Considering these observations, it can be said that the DWVG enhance convective heat transfer over a fin by reducing the wake region.

Fundamental thermodynamic variables, the values of which are obtained via CFD analyses, are related with system parameters such as the heat transfer coefficient and head loss coefficient. The following expressions delineate these relationships. The heat transfer coefficient is related with the temperature difference as follows:

$$h = \frac{Q}{(A_c + A_{fin})\Delta T_{LM}} \tag{13}$$

where Q and ΔT_{LM} represent the total heat transfer rate and log-mean temperature difference and are obtained by the following expression:

$$Q = \rho C_p (L \times W \times V_{\max}) \left| T_{in} - T_{out} \right| \tag{14}$$

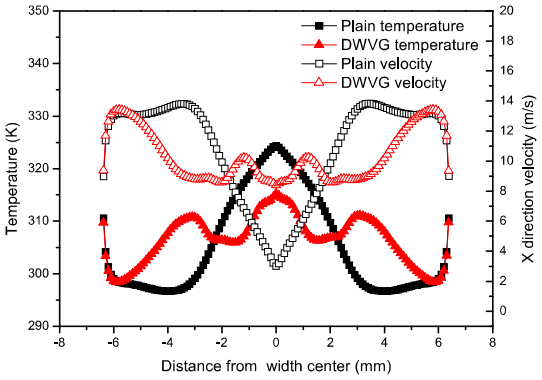

Figure 7 Air temperature and velocity at same line between tubes

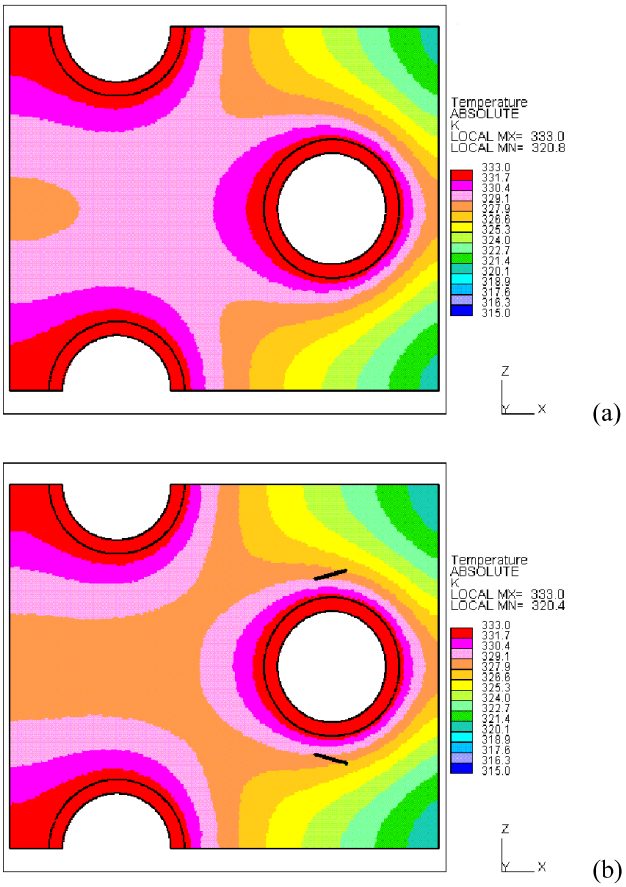

Figure 8 Fin surface temperature (Re=1295, V_{max}=8.07m/s) (a) Plain fin (b) DWVG

$$\Delta T_{LM} = \frac{(T_c - T_{in}) - (T_c - T_{out})}{\ln \left| \frac{T_c - T_{in}}{T_c - T_{out}} \right|} \tag{15}$$

where $V_{\max}$, T_{in}, and T_{out} represent the maximum velocity, inlet air temperature, and outlet air mean temperature, respectively. $V_{\max}$ is defined $U(A_f / A_{\min})$. T_{in} is constant in this work since we set it as a boundary condition at the entrance. However, T_{out} varies over the cross-sectional plane at the exit because it is influenced by heat transfer and fluid flow. An area average value was used in this work and is given as follows:

$$T_{out} = \frac{\int |u| T dA_f}{\int |u| dA_f} \tag{16}$$

where A_c, A_{fin}, L, W, T_c, and A_f represent the fin collar area, total fin area, length, width, fin collar temperature, and cross sectional area at the exit. The thermodynamic

properties used in the above equations are typically temperature

dependent. When we apply the above equations to temperature-varying situations, a mathematical average of properties evaluated at the lowest and the highest temperatures was used. Based on the CFD results we can calculate the convective heat transfer coefficient using the relationships of equations (13)~(16). Substituting this value for equations (10) and (11), the Colburn-j factor is obtained. Using the following equation, we can obtain the f-factor as well [12]

$$f = \frac{\Delta P}{(\rho \times V_{\max}^2 / 2)} \left(\frac{D_c}{4L} \right) \tag{17}$$

where ΔP and D_c are the pressure difference and characteristic length.

Fig. 9 shows the variation of the j-factor and f-factor with the frontal air velocity in a range of 0.5~20m/s. The frontal air velocity is represented in terms of Reynolds number. For the Reynolds number conversion, the hydraulic diameter was used as the characteristic length scale, and is equivalent to double the fin pitch. The j-factor for the DWVG fin is larger than that of the plain fin over the whole range evaluated. Moreover, an interesting trend was observed for the f-factor variation. The f-factor of the DWVG fin is higher than that of the plain fin, but the difference diminishes with an increase in Reynolds number in a range of Re<3000. When the Reynolds number increases beyond 3000, the f-factor of the DWVG fin even becomes smaller than that of the plain fin. In a range of Re>3000, the j-factor of the DWVG fin remains larger than that of the plain fin. These results appear to run contrary to the Reynolds analogy, which states that an enhanced surface will have a larger f-factor, as delineated by equation (11). However, the Reynolds analogy should not be expected to hold in the present situation. The Reynolds analogy is applicable to laminar and turbulent flows over a flat plate and a turbulent flow in a tube. However, this analogy does not hold when flow separation occurs. If we do not consider the tube and the wake region developed at the rear of the tube, the Reynolds analogy will be applicable. That is, the DWVG will generate longitudinal vortices and mix air to promote heat transfer. The DWVG will also act as a flow obstruction to produce an additional form loss as well. In the situation studied in the present work, however, there was an additional effect besides the vortex generation: reduction of the wake region due to flow acceleration between the tube and the

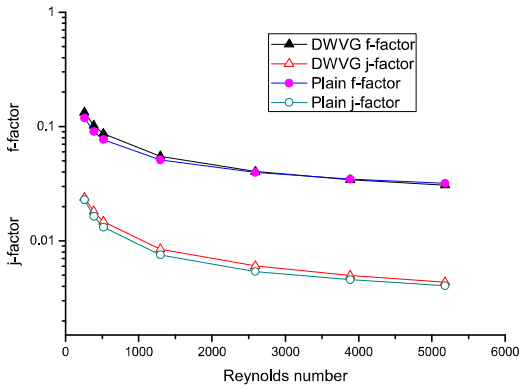

Figure 9 Value of f-and j-factor

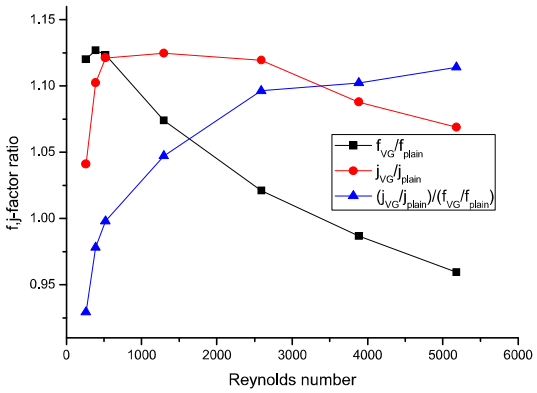

Figure 10 Ratio of f-and j-factor

DWVG itself. This reduction of the wake region decreases the form loss. Therefore, the DWVG in the present work plays a dual role of producing additional form loss and reducing form loss due to the wake. As the Reynolds number increases, the effect of the reduction of form loss becomes dominant over the effect of additional form loss. This explains how the f-factor of the DWVG fin becomes smaller than that of the plain fin.

Fig. 10 shows the ratio of the f-factor and j-factor of the DWVG fin with respect to that of the plain fin. The f-factor ratio increases in a low Reynolds number range but decreases steadily when the Reynolds number increases further. As the Reynolds number increases, the j-factor ratio is suddenly increased up to 1.13 and gradually decreases thereafter. Meanwhile, the f-factor ratio is reduced to less than 1 when the Reynolds number reaches 3000 or larger. Another interesting plot is the j-factor ratio over f-factor ratio. The Reynolds analogy states that an enhanced surface will have a value of '1'. The value obtained in previous fin design studies was usually less than 1. However, Fig. 11 shows that the ratio of the present DWVG fin increases beyond '1' as the Reynolds number increases. This implies that the present DWVG fin design will be more beneficial as the frontal air velocity increases.

CONCLUSION REMARKS

During the past decade numerous studies have been carried out to investigate the effect of vortex generators on heat transfer of fins. While it was consistently reported that the vortex generators enhanced the heat transfer performance, the pressure loss measurements did not yield agreement. In spite of a great deal of research having been conducted in this area, there remains a lack of understanding about the mechanisms contributing to heat transfer augmentation and a limited increase in pressure loss. In the present work, the air flow and heat transfer in a fin-tube heat exchanger have been analyzed using the CFD method in order to obtain a better phenomenological understanding of the effects of the delta winglet vortex generator on fin performance. The results show that flow acceleration between the delta winglet vortex generator and heat transfer tube delays the flow separation from

the tube. This delayed flow separation causes the wake region at the rear of the tube to shrink such that form loss is reduced and heat transfer is enhanced. Interestingly, the pressure loss of a fin having delta winglet vortex generators was evaluated to be even smaller than that of a plain fin while the heat transfer was enhanced at high air velocity or Reynolds number. Comparing the results of the f-factor and j-factor, it was also found that the performance of the DWVG fin is improved as the Reynolds number increases in terms of enhanced heat transfer and reduced pressure drop penalty.

REFERENCES

[1] K. Chang and P. Long, An experimental study of the airside performance of slit fin-and-tube heat exchangers under dry and wet conditions, *International Journal of Air-Conditioning and Refrigeration*, Vol 17(1), 2009, pp.7-14

[2] G.B. Schubauer and W.G. Spangenberg, Forced mixing in boundary layers, *Journal of Fluid Mechanics*, Vol 8, 1960, pp.10-31

[3] M. Fiebig, Vortices, generators and heat transfer, *Trans Institution of Chemical Engineers*, 1998, 76: Part A

[4] K. Torii, K. M. Kwak and K. Nishino, Heat transfer enhancement accompanying pressure-loss reduction with winglet-type vortex generators for fin-tube heat exchanger, *International Journal of Heat and Mass Transfer*, Vol 45, 2002, pp.3795-3801

[5] A. M. Jacobi and R. K. Shah, Heat transfer surface enhancement through the use of longitudinal vortices: A review of recent progress, *Experimental Thermal and Fluid Science*, Vol 11, 1995, pp.295-309

[6] M. Fiebig, A. Valencia and N.K. Mitra, Wing-type vortex generators for fin-and-tube heat exchangers, Experimental *Thermal and Fluid Science*, Vol 7, 1993, pp.287-295

[7] K. M. Kwak, K. Torii and K. Nishino, Heat transfer and pressure loss penalty for the number of tube rows of staggered finned-tube bundles with a single transverse row of winglets, *International Journal of Heat and Mass Transfer*, Vol 46, 2003, pp.175-180

[8] K. M. Kwak, K. Torii and K. Nishino, Simultaneous heat transfer enhancement and pressure loss reduction for finned-tube bundles with the first or two transverse rows of built-in winglets, *Experimental Thermal and Fluid Science*, Vol 29, 2005, pp.625-632

[9] B. R. Munson, D. F. Young and T. H. Okiishi, FUNDAMENTALS OF FLUID MECHANICS, 4th edition, WILEY, 2002

[10] A.A. Bastani, N.K. Mitra and G. Biswas, Numerical investigations on enhancement of heat transfer in a compact fin-and-tube heat exchanger using delta winglet type vortex generators, *Enhanced Heat Transfer*, Vol 6, 1999, pp.1-11

[11] F. P. Incropera, D. P. Dewitt, T. L. Bergman and A. S. Lavine, INTRODUCTION TO HEAT TRANSFER, 5th edition, WILEY, 2007

[12] S. Kakac, H. Liu, HEAT EXCHANGERS, CRC Press, 1998

[13] CD-adapco, STAR-CD Methodology manual, 2006

[14] Liting Tian, Yaling He, Yubing Tao, Wenquan Tao, A comparative study on the air side performance of wavy fin-and-tube heat exchanger with punched delta winglets in staggered and in-line arrangements, *International Journal of Thermal Sciences*, Vol 48, 2009, pp.1765-1776

[15] CD-adapco, STAR-CD, v4.06, 2008

[16] K. J. Kim and P. A. Durbin, Observations of the frequencies in a sphere wake and drag increase by acoustic excitation, *Physics of Fluids*, Vol 31, 1998, pp.3260-3265